Probing Furanose Ring Conformation by Gas-Phase Computational Methods: Energy Profile and Structural Parameters in Methyl β-D-Arabinofuranoside as a Function of Ring Conformation

Matthew T. Gordon, Todd L. Lowary,* and Christopher M. Hadad*

Department of Chemistry, Ohio State University, Columbus, Ohio 43210

lowary.2@osu.edu

Received March 22, 2000

The potential energy surface of methyl β-D-arabinofuranoside (**3**) has been studied by ab initio molecular orbital (HF/6-31G*) and density functional theory (B3LYP/6-31G*) calculations via minimization of the 10 possible envelope conformers. The partial potential energy surface identified that the global minimum and lowest energy northern conformer was E_2. In the HF calculations, ^2E was the most stable southern conformer, while the density functional theory methods identified ^4E as the local minimum in this hemisphere. Additional calculations at higher levels of theory showed that the B3LYP-derived energies of many of the envelope conformers of **3** are dependent upon the basis set used. It has also been demonstrated that B3LYP/6-31+G**//B3LYP/6-31G* single point energies are essentially the same as those obtained from full geometry optimizations at the B3LYP/6-31+G** level. The northern and southern minima of the B3LYP/6-31+G** surface are, respectively, the E_2 and ^2E conformers. The B3LYP/6-31G* geometries were used to study the relationship between ring conformation and various structural parameters including bond angles, dihedral angles, bond lengths, and interatomic distances.

Introduction

In a previous investigation,[1] we have reported ab initio and density functional theory (DFT) calculations of methyl α-D-arabinofuranoside (**1**, Scheme 1). These studies were undertaken in conjunction with our efforts directed toward understanding the conformation of polysaccharides containing D-arabinofuranose residues. Two such polymers, an arabinogalactan (AG) and a lipoarabinomannan (LAM), are present in the protective cell wall of the pathogenic organisms *Mycobacterium tuberculosis* and *Mycobacterium leprae*.[2] All of the arabinose and galactose in these polymers exist in the furanose ring form. Both AG and LAM play multifaceted roles in the infection and survival of these organisms in humans, and an understanding of their conformations will facilitate the rational design of drugs that act by inhibiting their biosynthesis.

Additionally, these studies may shed light on a more fundamental question. Namely, given that the furanose isomers are the least thermodynamically stable ring forms of most monosaccharides, why did mycobacteria evolve to synthesize cell wall polysaccharides comprised of furanosyl residues? While it has been suggested[3] that these oligosaccharides serve as flexible scaffolds that allow the proper organization of other cell wall components, no experimental support for this postulate exists. Critical to testing this hypothesis is a knowledge of the conformations of polyfuranosides and the monosaccharide residues of which they are comprised.

Scheme 1

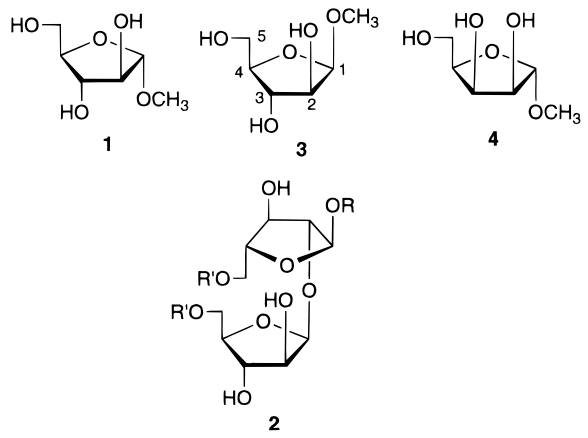

In comparison with the number of computational investigations on pyranose glycans,[4] such studies on furanose-containing oligosaccharides are less common. Molecular mechanics calculations have been reported for some monosaccharide furanose ring systems, including D-fructose,[5] D-psicose,[6] methyl α-L-arabinofuranoside,[7]

(1) Gordon, M. T.; Lowary, T. L.; Hadad, C. M. *J. Am. Chem. Soc.* **1999**, *121*, 9682.

(2) Brennan, P. J.; Nikaido, H. *Annu. Rev. Biochem.* **1995**, *64*, 29.

(3) Connell, N. D.; Nikaido H. Membrane Permeability and Transport in *Mycobacterium tuberculosis*. In *Tuberculosis: Pathogenesis, Prevention, and Control*; American Society for Microbiology Press: Washington, DC, 1994; pp 333−352.

(4) (a) Peters, T.; Pinto, B. M. *Curr. Opin. Struct. Biol.* **1996**, *6*, 710. (b) Homans, S. W. *New Compr. Biochem.* **1995**, *29a*, 67. (c) Rao, V. S. R.; Qasba, P. K.; Balaji, P. V.; Chandrasekaran, R. *Conformation of Carbohydrates*; Harwood Academic Publishers: Amsterdam, 1998. (d) Woods, R. J. *Glycoconjugate J.* **1998**, *15*, 209.

(5) French, A. D.; Dowd, M. D.; Reilly, P. J. *J. Mol. Struct. (THEOCHEM)* **1997**, *395−396*, 271.

(6) French, A. D.; Dowd, M. D. *J. Comput. Chem.* **1994**, *15*, 561.

10.1021/jo000426w CCC: $19.00
Published on Web 07/14/2000

methyl β-D-arabinofuranoside,[7] methyl α-D-ribofuranoside,[8] methyl β-D-ribofuranoside,[8] and the furanose forms of the D-aldo- and D-ketohexoses.[9] In some cases, these studies have been extended to oligosaccharides (e.g., sucrose[10] and glycans comprised of galactofuranosyl and fructofuranosyl residues[11,12]) and supported with NMR or X-ray crystallographic data.[7,8,10,11] Higher level ab initio and DFT calculations have also been carried out for some furanose monosaccharides, particularly D-ribofuranose,[13] 2-deoxy-D-*erythro*-pentofuranose,[13] the tetrofuranoses,[14] D-fructofuranose,[15] methyl α-D-arabinofuranoside,[1] and the furanose forms of the D-aldo- and D-ketohexoses.[9] The crystal structures of methyl α-D-arabinofuranoside, methyl α-D-lyxofuranoside, methyl α-D-xylofuranoside, and methyl β-D-ribofuranoside have recently been reported.[16] In the same paper, the solid-state geometries were used as the starting points for DFT calculations, which identified local minima of these ring systems that agreed well with the crystal structure data.

Furanose rings are flexible species and a model in which two conformers are present in equilibrium is generally used to describe their solution conformation. This concept can be conveniently visualized using the pseudorotational wheel (Scheme 2).[17] The two conformers present for a given ring are termed either north (N) or south (S) depending upon the hemisphere of the wheel in which they are located. Rather than interconverting via a planar ring structure, most furanose rings equilibrate via pseudorotation through a series of intermediate twist (T) and envelope (E) conformations.[18]

The majority of the D-arabinofuranose residues present in both AG and LAM are in the α-configuration. However, β-D-arabinofuranosyl residues are also present. These moieties (**2**, Scheme 1) are found at the periphery of the polysaccharides, and the primary hydroxyl group (OH_5) is usually substituted with other groups (mycolic acids or mannopyranosyl oligosaccharides) that are key players in the pathogenicity of the organism.[2] Therefore, in conjunction with our other structural[19] and synthetic[20] investigations on mycobacterial arabinofuranosides, we report here gas-phase ab initio and DFT calculations on the potential energy surface of methyl β-D-arabinofuranoside, **3** (Scheme 1).

Scheme 2

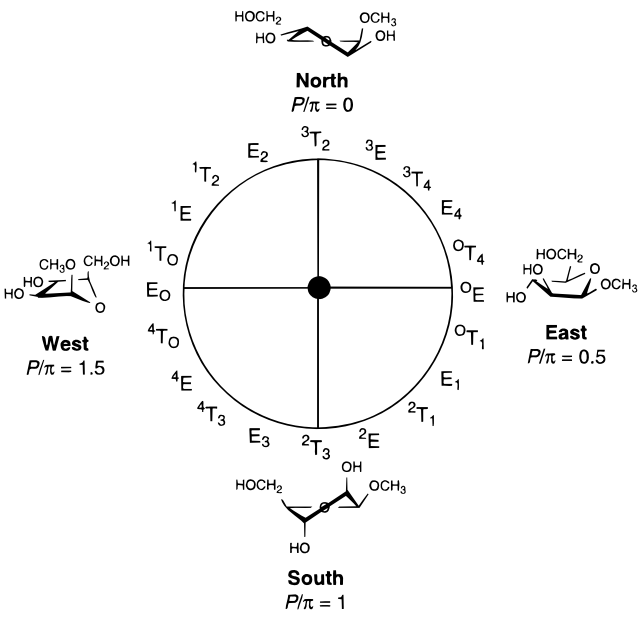

Pseudorotational Itinerary for Methyl β-D-arabinofuranoside

Methods

Ab initio molecular orbital and DFT calculations were conducted using Gaussian 94[21] as reported for **1**[1] and other furanose rings.[13,14,22] The 10 possible envelope conformations (^{3}E, E_4, ^{O}E, E_1, ^{2}E, E_3, ^{4}E, E_O, ^{1}E, and E_2) and the planar structure were optimized using both Hartree−Fock (HF)[23] and density functional theory (B3LYP)[24] calculations with the 6-31G* basis set. Each minimized envelope geometry was obtained by constraining a specific endocyclic torsion angle to 0° and allowing all of the other parameters to optimize. Con-

(7) (a) Cros, S.; Hervé du Penhoat, C.; Pérez, S.; Imberty, A. *Carbohydr. Res.* **1993**, *248*, 81. (b) Cros, S.; Imberty, A.; Bouchemal, N.; Hervé du Penhoat, C.; Pérez, S. *Biopolymers* **1994**, *34*, 1433.

(8) Gruza, J.; Koca, J.; Pérez, S.; Imberty, A. *J. Mol. Struct. (THEOCHEM)* **1998**, *424*, 269.

(9) Ma, B.; Schaefer, H. F., III; Allinger, N. L. *J. Am. Chem. Soc.* **1998**, *120*, 3411.

(10) (a) French, A.; Schafer, L.; Newton, S. Q. *Carbohydr. Res.* **1993**, *239*, 51. (b) Cassett, F.; Imberty, A.; Hervé du Penhoat, C.; Koca, J.; Pérez, S. *J. Mol. Struct. (THEOCHEM)* **1997**, *395*−*396*, 211. (c) Tran, V.; Brady, J. W. *Biopolymers*, **1990**, *29*, 961. (d) Tran, V. H.; Brady, J. W. *Biopolymers* **1990**, *29*, 977. (e) Hervé du Penhoat, C.; Imberty, A.; Roques, N.; Michon, V.; Mentech, J.; Descotes, G.; Pérez, S. *J. Am. Chem. Soc.* **1991**, *113*, 3720.

(11) (a) Waterhouse, A. L.; Horváth, K.; Liu, J. *Carbohydr. Res.* **1992**, *235*, 1. (b) Timmermans, J. W.; de Wit, D.; Tournois, H.; Leeflang, B. R.; Vliegenthart, J. F. G. *J. Carbohydr. Chem.* **1993**, *12*, 969.

(12) (a) Immel, S.; Schmitt, G. E.; Lichtenthaler, F. W. *Carbohydr. Res.* **1998**, *313*, 91. (b) Gohle, H.; Immel, S.; Lichtenthaler, F. W. *Carbohydr. Res.* **1999**, *321*, 96.

(13) (a) Podlasek, C. A.; Stripe, W. A.; Carmichael, I.; Shang, M.; Basu, B.; Serianni, A. S. *J. Am. Chem. Soc.* **1996**, *118*, 1413. (b) Church, T. J.; Carmichael, I.; Serianni, A. S. *J. Am. Chem. Soc.* **1997**, *119*, 8946. (c) Serianni, A. S.; Wu, J.; Carmichael, I. *J. Am. Chem. Soc.* **1995**, *117*, 8645. (d) Bandyopadhyay, T.; Wu, J.; Stripe, W. A.; Carmichael, I.; Serianni, A. S. *J. Am. Chem. Soc.* **1997**, *119*, 1737. (e) Cloran, F.; Carmichael, I.; Serianni, A. S. *J. Phys. Chem. A* **1999**, *103*, 3783.

(14) Serianni, A. S.; Chipman, D. M. *J. Am. Chem. Soc.* **1987**, *109*, 5297.

(15) Chung-Phillips, A.; Chen, Y. Y. *J. Phys. Chem. A* **1999**, *103*, 953.

(16) Evdokimov, A. G.; Kalb, A. J.; Koetzle, T. F.; Klooster, W. T.; Martin, J. M. L. *J. Phys. Chem. A* **1999**, *103*, 744.

(17) (a) Altona, C.; Sundaralingam, M. *J. Am. Chem. Soc.* **1972**, *94*, 8205. (b) Westhof, E.; Sundaralingam, M. *J. Am. Chem. Soc.* **1980**, *102*, 1493. (c) Harvey, S. C.; Prabhakaran, M. *J. Am. Chem. Soc.* **1986**, *108*, 6128. (d) Sundaralingam, M. *J. Am. Chem. Soc.* **1965**, *87*, 599.

(18) Westhof, E.; Sundaralingam, M. *J. Am. Chem. Soc.* **1983**, *105*, 970.

(19) D'Souza, F. W.; Ayers. J. D.; McCarren, P. R.; Lowary, T. L. *J. Am. Chem. Soc.* **2000**, *122*, 1251.

(20) (a) Ayers, J. D.; Lowary, T. L.; Morehouse, C. B.; Besra, G. S. *Bioorg. Med. Chem. Lett.* **1998**, *8*, 437. (b) D'Souza, F. W.; Cheshev, P. E.; Ayers, J. D.; Lowary, T. L. *J. Org. Chem.* **1998**, *63*, 9037. (c) Subramaniam, V.; Lowary. T. L. *Tetrahedron* **1999**, *55*, 5965. (d) D'Souza, F. W.; Lowary, T. L. *Org. Lett.* **2000**, *2*, 1493.

(21) Frisch, M. J.; Trucks, G. W.; Schlegel, H. B.; Gill, P. M. W.; Johnson, B. G.; Robb, M. A.; Cheeseman, J. R.; Keith, T.; Petersson, G. A.; Montgomery, J. A.; Raghavachari, K.; Al-Laham, M. A.; Zakrzewski, V. G.; Ortiz, J. V.; Foresman, J. B.; Cioslowski, J.; Stefanov, B. B.; Nanayakkara, A.; Challacombe, M.; Peng, C. Y.; Ayala, P. Y.; Chen, W.; Wong, M. W.; Andres, J. L.; Replogle, E. S.; Gomperts, R.; Martin, R. L.; Fox, D. J.; Binkley, J. S.; Defrees, D. J.; Baker, J.; Stewart, J. P.; Head-Gordon, M.; Gonzalez, C.; Pople, J. A. *Gaussian 94, Revision D.3*; Gaussian, Inc.: Pittsburgh, PA, 1995.

(22) (a) Garrett, E. C.; Serianni, A. S. In *Computer Modeling of Carbohydrate Molecules*; French, A. D., Brady, J. W., Eds.; ACS Symposium Series 430; American Chemical Society: Washington, DC, 1990; pp 91−119. (b) Garrett, E. C.; Serianni, A. S. *Carbohydr. Res.* **1990**, *206*, 183.

(23) Hehre, W. J.; Radom, L.; Schleyer, P. v. R.; Pople, J. A. *Ab initio Molecular Orbital Theory*; Wiley-Interscience: New York, 1986, and references therein.

(24) (a) Becke, A. D. *Phys. Rev. A* **1988**, *38*, 3098. (b) Becke, A. D. *J. Chem. Phys.* **1993**, *98*, 5648. (c) Lee, C.; Yang, W.; Parr, R. G. *Phys. Rev. B* **1988**, *37*, 785.

Scheme 3

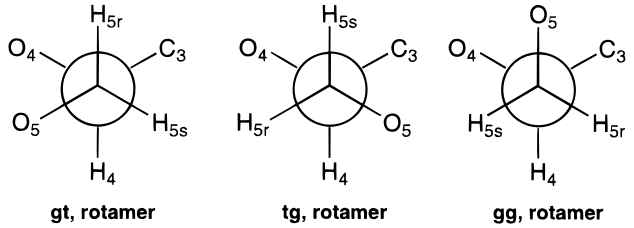

straint of two endocyclic torsion angles ($O_4-C_1-C_2-C_3$ and $C_4-O_4-C_1-C_2$) at 0° provided the planar conformer. The choice of exocyclic torsion angles was arbitrary except for the C_1-O_1 bond, which was initially chosen to maximize the *exo*-anomeric effect,[25] and the C_5-C_4 bond, which was placed in each of three staggered conformations: gg, gt, or tg (Scheme 3). A full surface scan, requiring the optimization of 2430 unique structures, was impractical as a result of available computer resources. However, a number of starting geometries were used for each envelope conformation to ensure location of the true minimum energy structure. As in previous investigations,[1,13,14,22] no attempt was made to include solvation through either the inclusion of explicit solvent molecules or dielectric fields.

Higher level single point energy calculations (HF, MP2, MP3, and B3LYP levels) were carried out using the 6-31+G**, 6-311+G**, and 6-311+G(2d,2p) basis sets.[23] All basis sets used six Cartesian *d* functions. Geometry optimizations were also done for some conformers at the B3LYP/6-31+G** level. Included in the discussion below is an analysis of the dependence of various structural parameters on conformation, which was done using the B3LYP/6-31G* optimized geometries; graphs of these parameters obtained from the HF/6-31G* optimizations are found in the Supporting Information. In the following discussion, *P* refers to the pseudorotational phase angle as defined in ref 17a.

Results and Discussion

Conformational Energy Profile. For **3**, HF/6-31G* and B3LYP/6-31G* optimizations identified a northern hemisphere conformer (E_2, $P/\pi = 1.9$) as the global minimum (Figure 1, Table 1). Although uniformity between both computational methods was observed for the relative energy of the N conformer, the identity of the southern minimum was dependent upon the level of theory. The relative energies for each envelope conformer are detailed in Table 1. While the HF calculations yielded ^2E ($P/\pi = 0.9$) as the southern minimum, the B3LYP optimizations identified ^4E ($P/\pi = 1.3$) as the local minimum in the southern hemisphere. At the B3LYP level, for each envelope conformer the preferred staggered orientation about the C_5-C_4 bond was gg. At HF, gg was favored in all conformers except ^2E and E_3 in which the gt rotamer was of lowest energy.

Gas-phase calculations of carbohydrates are complicated by the multiple hydrogen bonding interactions that are possible.[9,26–29] To probe the treatment of these interactions as a function of level of theory and basis set, Lii, Ma, and Allinger have recently reported a computational study of the linear water dimer.[27] This work was prompted by their previous work[9] on the conformational energies of D-hexoses, which demonstrated poor agreement between MM3(96) and B3LYP/6-31G** (5d) energies.

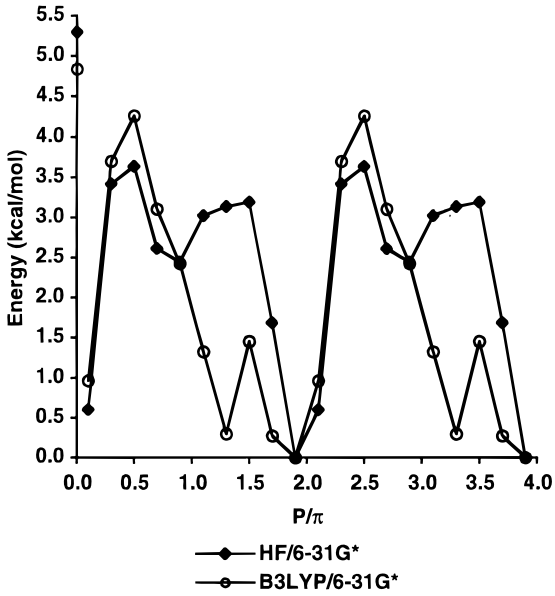

Figure 1. Energy profile of **3** for the 10 envelope conformations at the indicated level of theory. One cycle is 0−2 P/π (radians), where 0.1 $P/\pi = {}^3E$ (see Scheme 2). The energy of the planar form is placed on the *y* axis.

In their investigations on the water dimer,[27] Allinger and co-workers showed that when density functional theory (B3LYP) methods are used, it is essential to employ basis sets that include diffuse functions. Otherwise, there are significant basis set superposition errors (BSSEs) that must be corrected for. As expected, these errors were shown to be reduced as the size of the basis set was increased and diffuse functions were included. For example, in the case of B3LYP/aug-cc-VQZ calculations, the BSSE was 0.3% of the uncorrected energy. In contrast, when the 6-31G** basis set was used, the BSSE was 32.4%. Interestingly, the energy obtained at HF/6-31G**, in which electron correlation is neglected, was almost identical to that obtained at the B3LYP/aug-cc-VQZ level of theory.

The aug-cc-VQZ basis set is too large for use with systems substantially more complicated than the water dimer. Therefore, smaller basis sets must be employed in DFT calculations of carbohydrates and it was proposed[27] that the basis set of choice is 6-311++G(2d,2p). For BSSE reasons, it was proposed that intramolecular hydrogen bonding energies are overestimated when DFT methods are used with basis sets that do not include

(25) (a) Lemieux, R. U. *Pure Appl. Chem.* **1971**, *25*, 527. (b) Lemieux, R. U.; Koto, S. *Tetrahedron* **1974**, *30*, 1933.

(26) (a) Jebber, K. A.; Zhang, K.; Cassady, C. J.; Chung-Phillips, A. *J. Am. Chem. Soc.* **1996**, *118*, 10515. (b) Brown, J. W.; Wladkowski, B. D. *J. Am. Chem. Soc.* **1996**, *118*, 1190. (c) Barrows, S. E.; Dulles, F. J.; Cramer, C. J.; French, A. D.; Truhlar, D. G. *Carbohydr. Res.* **1995**, *276*, 219. (d) Cramer, C. J.; Truhlar, D. G. *J. Am. Chem. Soc.* **1993**, *115*, 5745. (e) Polavarapu, P. L.; Ewig, C. S. *J. Comput. Chem.* **1992**, *13*, 1255. (f) Barrows, S. E.; Storer, J. W.; Cramer, C. J.; French, A. D.; Truhlar, D. G. *J. Comput. Chem.* **1998**, *19*, 1111. (g) Csonka, G. I.; Csizmadia, I. G. *Chem. Phys. Lett.* **1995**, *243*, 419.

(27) Lii, J. H.; Ma, B.; Allinger, N. L. *J. Comput. Chem.* **1999**, *15*, 1593.

(28) Csonka, G.; Éliás, K.; Csizmadia, I. G. *Chem. Phys. Lett.* **1996**, *257*, 49.

(29) (a) Csonka, G.; Éliás, K.; Csizmadia, I. G. *J. Comput. Chem.* **1996**, *18*, 330. (b) Csonka, G.; Éliás, K.; Kolossváry, I.; Sosa, C. P.; Csizmadia, I. G. *J. Phys. Chem. A* **1998**, *102*, 1219.

Table 1. Energy Profile for Methyl β-D-Arabinofuranoside (3)[a,b]

		^3E	E_4	^OE	E_1	^2E	E_3	^4E	E_O	^1E	E_2	planar
HF	6-31G* (optimized)	0.6	3.4	3.6	2.6	2.4	3.0	3.1	3.2	1.7	0.0	5.3
	6-31+G**	0.1	2.5	2.6	2.7	4.1	5.3	5.2	3.5	1.8	0.0	4.8
	6-311+G**	0.0	2.3	2.4	2.7	4.2	5.6	5.4	3.6	2.0	0.1	4.9
	6-311+G(2d,2p)	0.2	2.5	2.6	2.7	4.4	5.3	5.4	3.8	2.0	0.0	5.0
MP2	6-31+G**	1.1	4.3	4.4	3.0	3.6	3.1	2.2	2.2	0.7	0.0	5.7
	6-311+G**	0.9	3.9	3.7	2.6	3.5	3.2	2.2	2.4	0.9	0.0	5.6
	6-311+G(2d,2p)	1.2	4.2	4.2	3.0	3.5	2.7	1.6	2.1	0.7	0.0	5.7
MP3	6-31+G**	0.9	3.8	3.9	2.8	3.6	3.5	2.7	2.4	0.9	0.0	5.3
	6-311+G**	0.7	3.3	3.2	2.4	3.5	3.5	2.7	2.5	1.1	0.0	5.1
B3LYP	6-31G* (optimized)	1.0	3.7	4.3	3.1	2.4	1.3	0.3	1.5	0.3	0.0	4.7
	6-31+G**	0.6	2.7	3.1	3.1	3.2	3.5	2.6	1.8	0.5	0.0	4.2
	6-31+G** (optimized)	0.5	2.7	3.1	3.1	3.2	3.5	2.6	1.8	0.5	0.0	4.2
	6-311+G**	0.4	2.5	2.9	3.3	3.4	3.6	2.6	1.8	0.4	0.0	4.2
	6-311+G(2d,2p)	0.6	2.7	3.0	3.3	3.5	3.4	2.6	1.9	0.5	0.0	4.2

[a] Relative energies are in kcal/mol at the bottom of the well. [b] Unless otherwise indicated, all energies are from single point calcuations using the B3LYP/6-31G* optimized geometries.

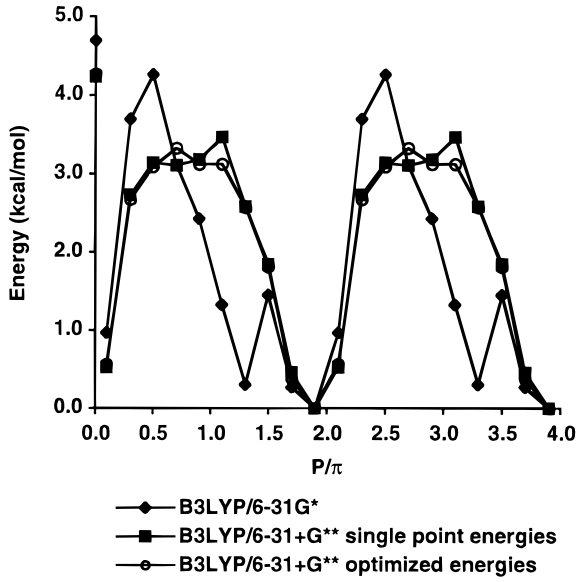

Figure 2. Comparison of the B3LYP/6-31G* (optimized, solid diamonds), B3LYP/6-31+G** (optimized, open circles), and B3LYP/6-31+G** (single point, solid squares) energies for all 10 envelope conformers of **3**. The energy of the planar form is placed on the *y* axis.

diffuse functions. Similar studies by Csonka and co-workers on β-D-glucopyranose[28] and α-L-fucopyranose[29] have also stressed the importance of using basis sets with diffuse functions in DFT calculations of carbohydrates, and convergence of energetic trends appear to be reached with 6-31+G* basis sets or larger.

To further probe the potential energy surface of **3**, additional calculations employing basis sets with diffuse functions have been carried out. It was our hope that these studies would resolve the discrepancy between the HF/6-31G* and B3LYP/6-31G* energies illustrated in Figure 1. Our first concern was to determine if reliable energies could be obtained from single point energy calculations or whether more time-consuming geometry optimizations are necessary. Accordingly, for each envelope we initially took the lowest energy B3LYP/6-31G* geometry (all possessed a gg orientation about the C_5-C_4 bond) and did full geometry optimizations at the B3LYP/6-31+G** level. These optimized energies, as well as their single point counterparts, are shown in Table 1 and Figure 2. *It is clear that the single point energy trends using the B3LYP/6-31G* geometries reproduces the same qualitative and quantitative trends as full geometry optimizations at the B3LYP/6-31+G** level.* In addition, the conformer geometries obtained from the B3LYP/6-31G* and B3LYP/6-31+G** optimizations are very similar (See Table S1 in Supporting Information). It appears, therefore, that the B3LYP/6-31G* method provides reliable geometries and that full geometry optimizations with larger basis sets are not necessary. Consequently, we have used the B3LYP/6-31G* geometries for all further single point energy calculations.

As indicated in Table 1, single point energies have been calculated at a number of theoretical levels employing the 6-31+G**, 6-311+G**, and 6-311+G(2d,2p) basis sets. With regard to the B3LYP energies, convergence is reached with the 6-31+G** basis set. Similar results have been reported for BP density functional theory calculations on α-L-fucopyranose.[29b] For some conformers of **3**, there is, however, a substantial qualitative and quantitative difference between these single point energies and those obtained from the B3LYP/6-31G* optimizations. This observation is in accord with the previously described results of Allinger and co-workers, which demonstrated that basis sets with diffuse functions must be used to obtain reliable energies from DFT calculations of carbohydrates.[27] Similarly, for the HF, MP2, and MP3 single point energies, good agreement across the three basis sets is seen for all conformers, and convergence is reached with the 6-31+G** basis set. *On the basis of these results, we propose that for* ***3*** *the 6-31+G** basis set provides reliable energies for all conformers.* For the following discussion, we focus on the B3LYP-derived potential energy surface.

All B3LYP calculations, regardless of basis set, identify E_2 ($P/\pi = 1.9$) as the lowest energy N conformer and the global minimum. This conformer is stabilized by the pseudoaxial orientation of the OCH_3 group at C_1, via the anomeric effect. Furthermore, the groups at C_2, C_3, and C_4 are pseudoequatorial, which would be favored on the basis of steric arguments. Moreover, in this conformer the dihedral angle between O_1 and O_2 is at a maximum, thus minimizing torsional strain between these two substituents, which have a 1,2-*cis* relationship on the ring (see below). On the other hand, the identity of the S conformer is dependent upon the basis set. At B3LYP/6-31G* a well-defined minimum is present, ^4E ($P/\pi = 1.3$), but this same conformer is not a minimum at the higher levels. Instead, in these more expensive calculations (Figure 2, Table 1), there appears to be, at best, a minimum at ^2E ($P/\pi = 0.9$) in a very shallow energy well.

Table 2. B3LYP/6-31+G//B3LYP/6-31G* Energies of the Three C_5-C_4 Bond Staggered Rotamers of Methyl β-D-Arabinofuranoside (3)[a]**

		rotamer[b]		
conformer	P/π	gg	gt	tg
^3E	0.1	0.6	1.1	3.1
E_4	0.3	2.7	3.3	5.3
^OE	0.5	3.1	3.7	4.7
E_1	0.7	3.3	3.3	4.5
^2E	0.9	3.4	2.9	4.0
E_3	1.1	3.5	3.1	4.1
^4E	1.3	2.6	3.7	5.4
E_O	1.5	1.8	3.2	4.5
^1E	1.7	0.4	1.5	3.2
E_2	1.9	0.0	0.2	2.3
planar		4.3	3.2	6.2

[a] Relative single point energies are in kcal/mol at the bottom of the well. [b] See Scheme 3 for rotamer definitions.

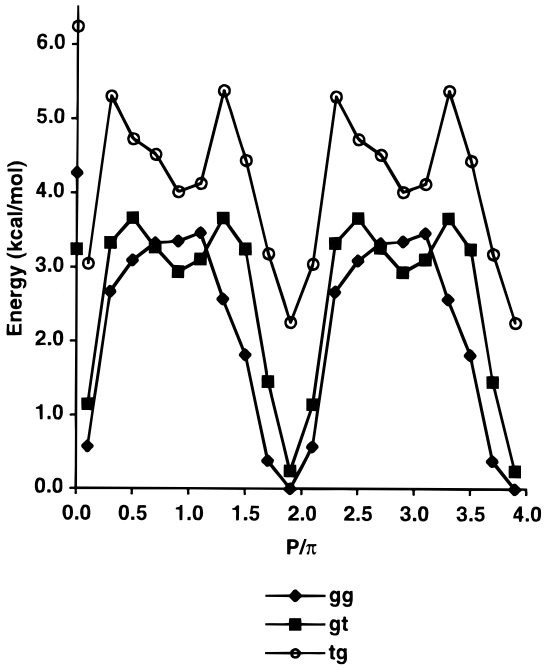

Figure 3. B3LYP/6-31+G** single point energies as a function of C_5-C_4 rotamer. The energy of the planar form is placed on the *y* axis.

The lack of a well-defined S conformer in the B3LYP-derived potential energy surface with the larger basis sets prompted us to reinvestigate geometries of **3** possessing additional staggered orientations about the C_5-C_4 bond. In the B3LYP/6-31G* optimized structures, the most favored orientation about the C_5-C_4 bond is gg, and these geometries were initially used to calculate the B3LYP/6-31+G**, B3LYP/6-311+G**, and B3LYP/311+G(2d,2p) single point energies. To address the possibility that with the larger basis set other C_5-C_4 rotamers (gt or tg) might be of lower energy than gg, we have carried out single point (B3LYP/6-31+G**) calculations of all three possible staggered rotamers for each ring conformer. These results (Table 2, Figure 3) show that, for two ring conformers found in the southern hemisphere (^2E, $P/\pi = 0.9$ and E_3, $P/\pi = 1.1$), the lowest energy conformer possesses the gt, not gg, orientation about the C_5-C_4 bond. Although the energy differences are small, when these two gt conformers are included in place of their gg counterparts, the potential energy surface shows a more pronounced energy minimum in the southern hemisphere at ^2E. *It appears, therefore, that when moving to larger basis sets it is important that all three possible C_5-C_4 bond rotamers be considered, not just those that are minima at lower levels of theory.*

It is interesting to note that the HF/6-31G* optimizations correctly identified that for the ^2E and E_3 conformers, the preferred orientation about the C_5-C_4 bond is gt. This suggests that, despite neglecting electron correlation, HF does a reasonable job of predicting the preferred conformers of this ring system. This result is in accord with the previously described work on the water dimer.[27] The good agreement between HF/6-31G* energies and those obtained from higher level calculations (DFT or MP2) on carbohydrates has been previously reported.[26b,28,29]

Conversion between the global minimum and other local minima can occur through pseudorotation via an eastern or western route or by inversion through the planar ring form.[17,18] In the case of **1**, pseudorotation through the eastern pathway was preferred by 3−5 kcal/mol depending upon the level of theory used.[1] For **3**, the B3LYP/6-31+G** single point energies identify a slight preference (0.2 kcal/mol) for the western pathway (Figure 3). Interestingly, the planar conformer possessing the gt orientation about the C_5-C_4 bond is of essentially equal energy to the barrier to pseudorotation through the east (E_1, $P/\pi = 0.7$).

In earlier work,[7a] Imberty and co-workers have reported MM3 calculations on **3**, which identified $^3T_2$ ($P/\pi = 0.0$) and $^2T_3$ ($P/\pi = 1.0$) as the N and S minima, respectively, with the former being the global minimum. Pseudorotation through the east was found to be favored. With the smaller basis set, our HF results are consistent with their findings in that envelopes (^2E or E_2) adjacent to these twist conformers are minima. Although poor agreement is observed with our B3LYP/6-31G* optimized results, when larger basis sets are used, the N and S minima are similar to the structures derived from molecular mechanics.

In sum, these results point to a conformational equilibrium heavily favoring the N conformer, E_2. This is perhaps not unexpected because the conformers lying in the southern hemisphere have a pseudoequatorially oriented OCH_3 at C_1. As a result, these conformers do not benefit from stabilization by the anomeric effect. Our NMR data on **3** also supports a model with the predominance of one conformer in solution. PSEUROT 6.2[30] analysis of the $^3J_{H,H}$ obtained from the ^1H NMR spectrum of **3** predicts an 99:1 E_2:^2E conformer ratio at equilibrium (see the Supporting Information for details on this calculation). These results are in accord with previous NMR studies of **3**.[31]

The potential energy surface of **3** is clearly much more complex than that of the α-isomer, **1**, in which the trends are consistent across all levels of theory.[1] This degree of complexity has not previously been seen in other systems investigated using the protocol employed here. It is noteworthy that although a number of ring systems have been studied in this manner,[1,13,14,22] this is the first in which three of the four possible ring substituents are on one face of the ring. Furthermore, with the exception of

(30) (a) *PSEUROT 6.2*; Gorlaeus Laboratories, University of Leiden. (b) de Leeuw, F. A. A. M.; Altona, C. *J. Comput. Chem.* **1983**, *4*, 428. (c) Altona, C. *Recl. Trav. Chem. Pays-Bas* **1982**, *101*, 413.

(31) Serianni, A. S.; Barker, R. *J. Org. Chem.* **1984**, *49*, 3292.

Table 3. Intramolecular Hydrogen Bonding in 3

			B3LYP/6-31G*			B3LYP/6-31+G**		
conformer	P/π	type[a]	C_5-C_4[b]	distance[c]	angle[d]	C_5-C_4[b]	distance[c]	angle[d]
^3E	0.1	$OH_5\cdots O_4$	gg	2.30	110.7	gg	2.42	106.0
		$OH_2\cdots O_1$		2.04	116.6		2.07	115.1
E_4	0.3	$OH_5\cdots O_4$	gg	2.29	110.3	gg	2.40	105.7
		$OH_2\cdots O_1$		1.94	119.8		1.98	118.9
^OE	0.5	$OH_5\cdots O_4$	gg	2.30	110.8	gg	2.41	106.4
		$OH_2\cdots O_1$		2.00	117.6		2.04	115.7
E_1	0.7	$OH_5\cdots O_4$	gg	2.47	108.3	gg	2.51	106.3
		$OH_2\cdots O_1$		2.07	115.7		2.13	112.8
^2E	0.9	$OH_5\cdots O_4$	gg	*e*	*e*	gt	2.37	106.9
		$OH_5\cdots O_2$		1.90	153.7		*e*	*e*
		$OH_2\cdots O_1$		1.98	118.0		2.07	115.2
E_3	1.1	$OH_5\cdots O_4$	gg	2.33	106.5	gt	2.38	108.0
		$OH_2\cdots O_5$		1.87	153.7		*e*	*e*
		$OH_5\cdots O_1$		2.31	135.6		*e*	*e*
		$OH_2\cdots O_1$		*e*	*e*		1.99	117.0
^4E	1.3	$OH_5\cdots O_1$	gg	1.89	145.7	gg	1.96	142.8
		$OH_2\cdots O_5$		1.98	147.2		2.08	144.2
E_O	1.5	$OH_5\cdots O_1$	gg	1.92	152.3	gg	1.96	152.2
		$OH_2\cdots O_1$		2.09	113.2		2.08	114.8
^1E	1.7	$OH_5\cdots O_1$	gg	1.97	156.8	gg	2.01	154.8
		$OH_2\cdots O_1$		2.12	114.9		2.16	112.9
E_2	1.9	$OH_5\cdots O_4$	gg	2.44	109.4	gg	2.51	106.4
		$OH_5\cdots O_1$		2.44	143.4		2.58	136.7
		$OH_2\cdots O_1$		2.14	114.5		2.17	112.6

[a] Hydrogen bond defined as the hydrogen donor···oxygen acceptor. [b] Rotamer about the C_5-C_4 bond. [c] H···O distance in Å. [d] O−H···O angle in degrees. [e] No H-bond seen in this conformer at this level of theory as a result of the basis set dependence of the most favored C_5-C_4 rotamer.

1[1] and the tetrofuranoses,[14] the effect of basis set on conformational energies has not previously been investigated in detail. However, it should be mentioned that recent calculations[16] on methyl α-D-lyxofuranoside, **4** (Scheme 1) in which the solid-state structure was used as the starting point for geometry optimizations, showed that larger, more flexible basis sets provided results that were in better agreement with experiment than small basis sets. In **4**, as in **3**, three of the substituents are on the same face of the ring.

Importance of Intramolecular Hydrogen Bonding. It is well understood that in the gas phase, carbohydrates are stabilized by the formation of intramolecular hydrogen bonds.[9,26−29] Table 3 lists the hydrogen bonds present in the lowest energy envelope conformers of **3** optimized at the B3LYP/6-31G* and B3LYP/6-31+G** levels. Only the O···H distances and the O−H···O angles are listed in the table.[32] Although important in the gas phase, the significance of intramolecular hydrogen bonding interactions are likely to be reduced in aqueous media through solvation of the hydroxyl groups. Clearly, in conformationally flexible ring systems such as these, if intramolecular hydrogen bonding provides differential stabilization of one or more conformers, the possibility exists that the energetic trends may be of limited utility in interpreting the behavior of these ring systems in solution. It should be appreciated, however, that Cramer and Truhlar have shown that for 1,2-ethanediol, intramolecular hydrogen bonding exists in both gas-phase and solution structures and the solvation effect is a small perturbation of the gas-phase effect.[33]

An analysis of the data in Table 3 shows that for the B3LYP/6-31+G** geometries of **3**, in nine of the ten envelope conformers there are two intramolecular hydrogen bonds present; however, in the global minimum structure, E_2, there are three. We were therefore concerned that the energy of the E_2 conformer was artificially low as a result of the presence of an additional transannular hydrogen bond between OH_5 and O_1 (Table 3). This transannular hydrogen bond might be anticipated to be moderately strong given the O···H distance (2.58 Å) and the O−H···O angle (136.7°).[34] The other two H-bonds present in the E_2 conformer of **3** ($OH_5\cdots O_4$ and $OH_2\cdots O_1$) are very similar to those found in conformers lying in the southern hemisphere (e.g., E_1), which are approximately 3−3.5 kcal/mol higher in energy.

However, we do not believe that the energy of the E_2 conformer is significantly biased by the formation of an additional transannular hydrogen bond. For **3**, the formation of transannular hydrogen bonds is only possible when the orientation about the C_5-C_4 bond is gg. Therefore, for a given conformer, a comparison of the energies of the gg and gt rotamers (Table 2, Figure 3) will provide insight into the importance of these H-bonding interactions and in turn the possibility of differential conformer stabilization. *For the E_2 conformer, the gt rotamer is only 0.2 kcal/mol higher in energy than the gg rotamer. Therefore, it is clear that the formation of this "extra" hydrogen bond does not appreciably stabilize this ring conformer relative to the others.*[35] While for some conformers there are significant energy differences between these gg and gt rotamer isomers, the qualitative trends for both are similar. For tg rotamers, the trend, while qualitatively similar to those of their gg and gt counterparts, is of higher energy. This is to be expected because in the gg and gt rotamers, gauche interactions[36] with the ring oxygen are possible (in addition to the formation of intramolecular hydrogen

(32) The distances between the heavy atoms can be obtained from the Cartesian coordinates in the Supporting Information.

(33) Cramer, C. J.; Truhlar, D. G. *J. Am. Chem. Soc.* **1994**, *116*, 3892.

(34) Jeffrey, G. A. *An Introduction to Hydrogen Bonding*; Oxford Press: New York, 1997; pp 11−32.

(35) $OH_5\cdots O_4$ and $OH_2\cdots O_1$ hydrogen bonds are present in both the E_2 tg and E_2 gg conformers.

(36) Wolfe, S. *Acc. Chem. Res.* **1972**, *5*, 102.

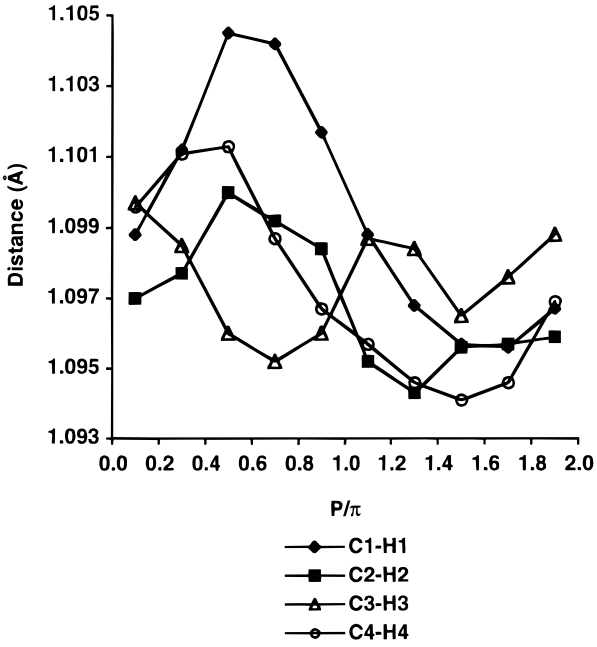

Figure 4. The dependence of C−H exocyclic bond distances on ring conformation of **3** at B3LYP/6-31G*.

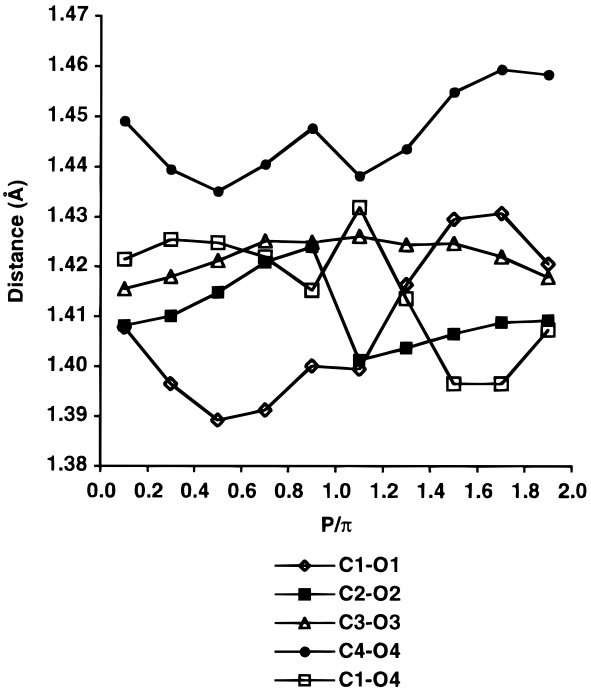

Figure 5. The dependence of C−O exocyclic bond distances on ring conformation of **3** at B3LYP/6-31G*.

bonds), whereas in the case of the tg rotamer, these interactions are not possible.

In aqueous solution, the gg:gt:tg ratio is 34:55:11,[37] which is in poor agreement with the gas-phase populations described here. A plausible explanation for this discrepancy arises from the difference in dipole moments of these two structures. The calculated dipole moments for the E_2 gg and E_2 gt conformers are 2.37 and 3.14 D, respectively. It would therefore be anticipated that on going from the gas phase to a polar solvent, the conformer with the larger dipole would be favored. A previous experimental investigation[38] in which C_5-C_4 rotamer populations in D-glucose derivatives was studied as a function of solvent polarity revealed similar trends. Furthermore, ab initio investigations[26c,d,f] of D-glucose in which solvation was been considered through a solvation model and has shown that the gt rotamer is of lowest energy due to better solvation of this conformational isomer.

Structural Parameters. As demonstrated in other furanose ring systems, various structural parameters in **3** (i.e., bond distances, bond angles, dihedral angles, and interatomic distances) are related to envelope conformation. A detailed understanding of these relationships is needed to facilitate NMR investigations of molecules containing β-D-arabinofuranosyl rings, and the relationship between the B3LYP/6-31G* parameters and ring conformation is discussed below.

Bond Lengths. The C−H bond distances involving the ring carbons of **3** are conformationally sensitive, varying from 0.006 to 0.01 Å (Figure 4). The trends observed are consistent with previous studies[1,13,14] that found that C−H bond lengths depend on their orientation; in particular, C−H bonds are slightly longer when pseudoaxial. For example, in the case of **3**, the C_3-H_3 bond is shortest in the conformers in which the bond is pseudoequatorial, e.g., E_1 ($P/\pi = 0.7$), ^2E ($P/\pi = 0.9$), and E_3 ($P/\pi = 1.1$), and longest when pseudoaxial as in E_2 ($P/\pi = 1.9$) and ^3E ($P/\pi = 0.1$). The bond distances for the diastereotopic hydrogens on C_5 are insensitive to conformation (see Supporting Information).

The lengths of the exocyclic C−O bonds also have an orientational dependence (Figure 5). The C_3-O_3 bond length varies by 0.009 Å across all conformers, and the C_2-O_2 bond distance is slightly more variable (0.01 Å). This is similar to the behavior of these structural parameters in **1**.[1] However, in **3**, the C_2-O_2 bond length varies over a larger range than in **1** and may reflect the number of hydrogen-bonding possibilities that are available to O_2. In other words, this bond may shorten or lengthen to form better hydrogen bonds. Conversely, OH_3 does not participate in hydrogen bonding interactions in any conformer (Table 3), and as expected the length of the C_3-O_3 bond is relatively constant regardless of conformation.

The C_1-O_1 bond distance is the C−O bond length that is most sensitive to conformation. As a result of the anomeric effect, there is an inverse relationship between the lengths of the C_1-O_4 and C_1-O_1 bonds (Figure 5). In those conformations where the anomeric oxygen is pseudoaxial (e.g., ^1E, $P/\pi = 1.7$), maximum $n \rightarrow \sigma^*$ donation from the ring oxygen results in a lengthening of the C_1-O_1 bond and a concomitant decrease in the C_1-O_4 bond distance. In conformations where the C_1-O_1 bond is pseudoequatorial (e.g., $^O E$, $P/\pi = 0.5$), opposite trends are observed.

Previous calculations on **1** have indicated that the minimum bond distances for a particular C−C bond occur in envelopes in which one of the carbons is displaced from the plane of the ring.[1] Although the origin of this effect is unclear, similar trends are seen in **3** (Figure 6). Bond length maxima occur, as they did in **1**, for the bond opposite to the atom above or below the plane. The

(37) Wu, G. D.; Serianni, A. S.; Barker, R. *J. Org. Chem.* **1983**, *48*, 1750.
(38) Rockwell, G. D.; Grindley, T. B. *J. Am. Chem. Soc.* **1998**, *120*, 10953.

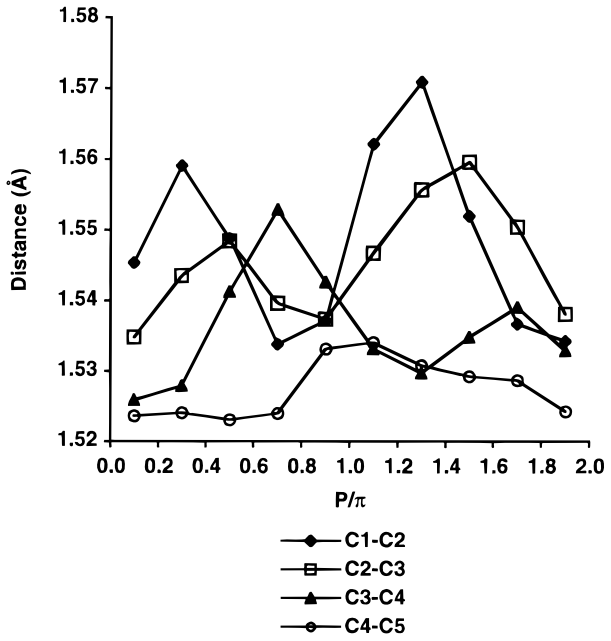

Figure 6. The dependence of C−C endocyclic bond distances on ring conformation of **3** at B3LYP/6-31G*.

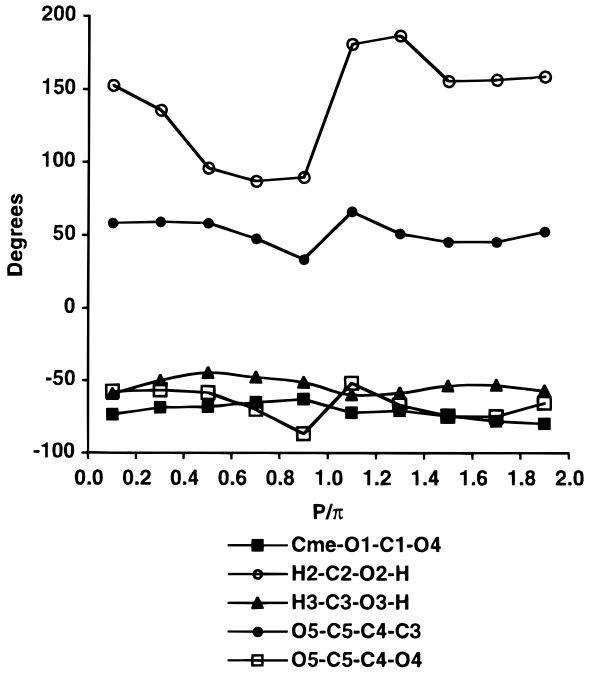

Figure 7. The dependence of C−O dihedral angles as a function of ring conformation of **3** at B3LYP/6-31G*.

C_3-C_4 bond length is at a maximum in the E_1 (P/π = 0.7) conformer in which the C_3-C_4 bond is opposite to C_1, the out-of-plane atom. Presumably this bond is longer because the groups in the bond opposite to the out-of-plane atom are necessarily eclipsed given their location in the plane of the envelope. Increasing this bond distance would be expected to minimize torsional strain. It would be expected, therefore, that the length of the C_1-C_2 bond would be especially long as both O_1 and O_2 are *cis* and hence eclipsing these (large, non-hydrogen) groups would be particularly unfavorable. Indeed, the length of the C_1-C_2 bond is on average longer than the other two intracyclic C−C bonds. Moreover, the longest C−C bond present in any conformer of **3** is the C_1-C_2 bond in ^4E (P/π = 1.3). Finally, in comparison with **1** where O_1 and O_2 are *trans* to each other on the ring, the C_1-C_2 bond in **3** is longer in all conformers (see Table S2 in the Supporting Information).

Dihedral Angles and Interatomic Distances. There is only limited flexibility about two of the three exocyclic C−O bonds (Figure 7). In the case of the C_1-O_1 bond, the $C_{Me}-O_1-C_1-O_4$ dihedral angle varies only between −63° and −80° as a consequence of the *exo*-anomeric effect. The $H_3-C_3-O_3-H$ angle is also insensitive to conformation and ranges between −45° and −60°. The preferred rotation about this bond is one in which the hydroxyl hydrogen is projected away from the ring. The behavior of this parameter in **3** is in marked contrast to **1**, in which this angle was conformationally sensitive. However in **1**, the anomeric methoxy group is located on the bottom face of the ring and hence in a position to form a transannular intramolecular hydrogen bond with OH_3 ($OH_3\cdots O_1$) in some conformers. The formation of an analogous hydrogen bond in **3** is stereochemically impossible.

In contrast, the $H_2-C_2-O_2-H$ angle is sensitive to conformation, but the observed trend is difficult to rationalize. In **3**, OH_2 can form a hydrogen bond either to O_1 ($OH_2\cdots O_1$) or to O_5 ($OH_2\cdots O_5$) via a five- or seven-membered ring, respectively. In most of the conformers,

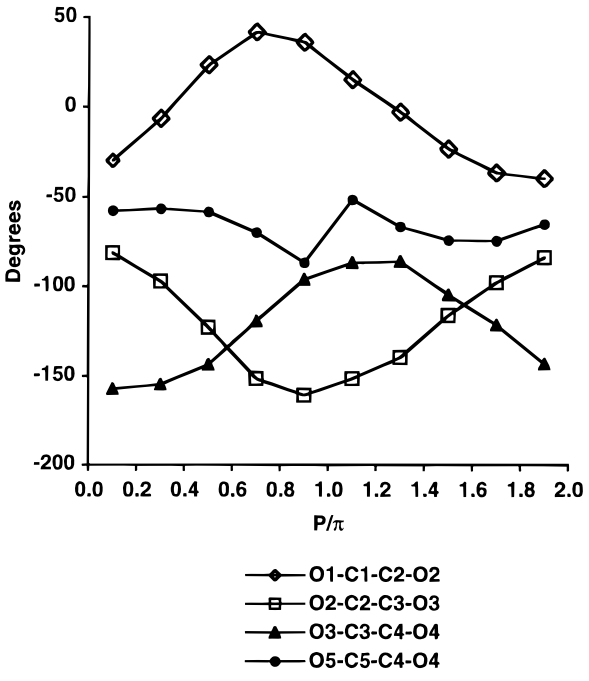

Figure 8. The dependence of O_x-O_y dihedral angles on ring conformation of **3** at B3LYP/6-31G*.

the $OH_2\cdots O_1$ bond is preferred, but in one (^4E), an $OH_2\cdots O_5$ bond is favored. We are uncertain why this conformer prefers to form a seven-membered ring hydrogen bond. Furthermore, there appears to be no relationship between the dihedral angle about the C_1-O_2 bond and hydrogen-bonding interactions.

The distances between the groups attached to the ring carbons vary as a function of envelope conformer, as illustrated in Figures 8 and 9, which show the conformational dependence of the O/O and H/H dihedral angles, respectively. Similar behavior has previously been reported for other furanose rings.[1,13,14] Related to the H/H

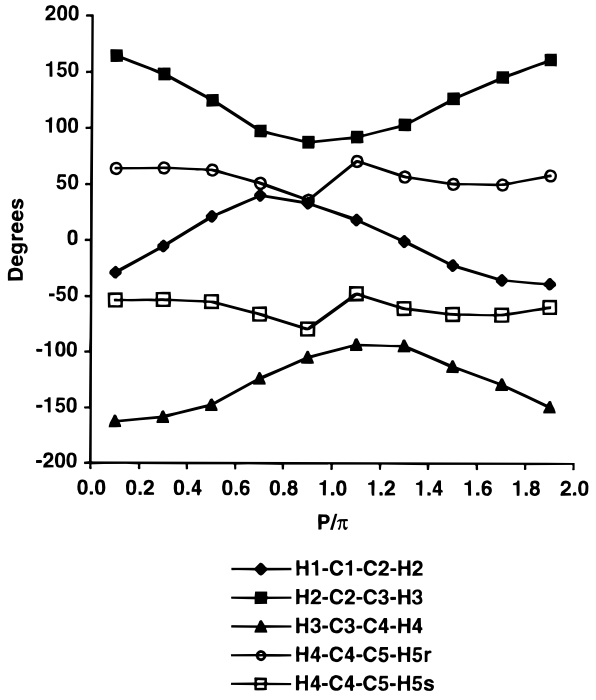

Figure 9. The dependence of H_x-H_y dihedral angles on ring conformation of **3** at B3LYP/6-31G*.

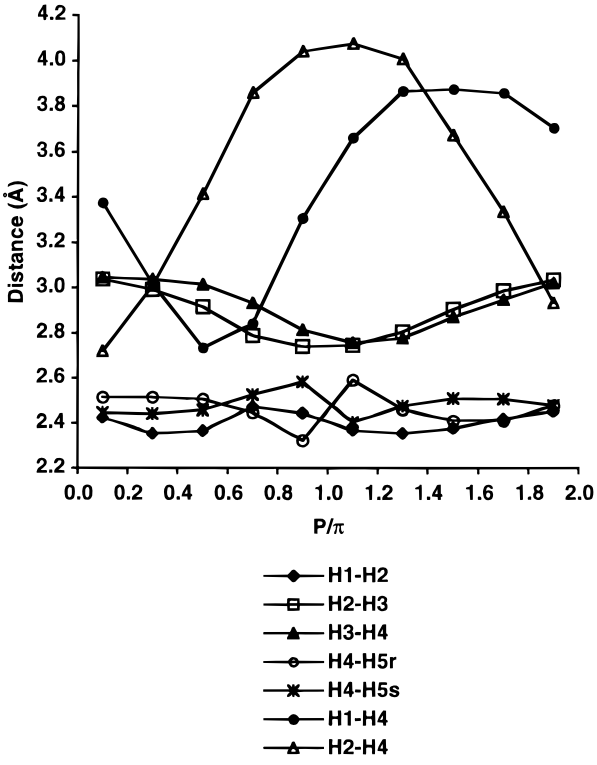

Figure 10. The dependence of H_x-H_y internuclear distances on ring conformation of **3** at B3LYP/6-31G*.

dihedral angles is the internuclear distance between the ring hydrogens. As illustrated in Figure 10, the distance between hydrogens on adjacent carbons varies little over all conformers (0.4 Å), but the distances spanned between hydrogens oriented 1,3-*cis* on the ring (H_1/H_4 and H_2/H_4) is greater than 1 Å.

Ring Puckering. In the idealized envelope geometries studied in these investigations, it is most convenient to describe ring puckering by measuring the angle that the out-of-plane atom makes with the plane rigorously defined by the other four atoms. However, in conformers lacking a well-defined plane (e.g., twists), this analysis is more difficult. Accordingly, the standard Cremer–Pople puckering amplitude[39] is generally used to define ring puckering. The degree of displacement of the out-of-plane atom from the plane of the other four atoms is shown in Table 4 along with the Cremer–Pople puckering amplitude. The minimum and maximum puckering occurs in the same conformer in both ring systems, E_O and E_1, respectively. In the least puckered conformer, E_O, the flattening of the ring likely arises from the steric strain between the C_4 hydroxymethyl group and the C_1 methoxy group, which are both pseudoaxial and hence forced into close proximity. The maximum puckering observed in the E_1 conformer of **3** is likely driven by the formation of a transannular hydrogen bond (in this case $OH_5\cdots O_2$). Increasing the ring puckering in this conformer would place O_2 more pseudoaxial and in a better position to hydrogen bond with OH_5.

Table 4. Ring Puckering in 3[a]

conformer	P/π[b]	out-of-plane[b]	Cremer–Pople[c,d]
^3E	0.1	22.6	0.368
E_4	0.3	20.1	0.315
^OE	0.5	21.0	0.331
E_1	0.7	23.7	0.377
^2E	0.9	21.0	0.336
E_3	1.1	19.6	0.316
^4E	1.3	20.9	0.329
E_O	1.5	16.3	0.256
^1E	1.7	18.7	0.293
E_2	1.9	21.4	0.344

[a] B3LYP/6-31G* optimized conformers. The C_5-C_4 torsion angle is gg in all cases except ^2E and E_3, which are tg. [b] Displacement angle (in deg) for the out-of-plane atom from the plane defined by the four other atoms. [c] Cremer–Pople puckering amplitude (in Å) as defined in ref 39. [d] The Cremer–Pople phase angle can be obtained by subtracting 90° from the Altona–Sundaralingam phase angles reported here.

Scheme 4

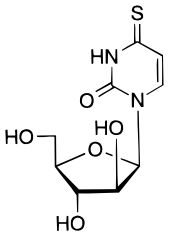

5

Comparison[1] of the puckering calculated for **1** with that of its crystal structure[16] revealed an almost identical displacement of the out-of-plane atom in both the crystalline and gas phases. Unfortunately, there are no reported crystal structures of β-D-arabinofuranosyl glycosides with which to compare our results. However, a number of crystal structures for β-D-arabinofuranosyl nucleotides have been solved. For those structures that crystallize with the sugar ring in an envelope conformation, there is a preference for either the ^2E or ^3E conformer. In the crystal structure[40] of **5** (Scheme 4), the ring adopts a ^3E conformation with C_3 being displaced 23.7° from the

(39) Cremer, D.; Pople, J. A. *J. Am. Chem. Soc.* **1975**, *97*, 1354.
(40) Saenger, W. *J. Am. Chem. Soc.* **1972**, *94*, 621.

plane of the ring (Cremer−Pople puckering, 0.387 Å). The degree of puckering predicted by our B3LYP/6-31G* calculations compare favorably with what is observed in the crystal; in the ^{3}E conformer of **3**, C_3 is displaced 22.6° from the plane (Cremer−Pople puckering, 0.368 Å). Table S3 and Scheme S1 in the Supporting Information contain additional examples comparing the out-of-plane puckering in the crystal structures of eleven β-D-arabinofuranosyl nucleotides, including **5**, with that of the appropriate envelope conformer of **3**. For these 11 nucleotides, the deviation between the out-of-plane puckerings in the crystal structure and gas-phase conformers range from 0° to 5.4° with an average deviation of 2.4°. For the Cremer−Pople puckerings, the range is 0.004−0.115 Å with an average deviation of 0.038 Å.

Conclusions

The ab initio and DFT calculations for the 10 unique envelope conformers of methyl β-D-arabinofuranoside (**3**) were carried out as part of a larger study directed toward understanding the conformational preferences of D-arabinofuranosyl rings.[1,18] Our conclusions are

(a) HF/6-31G* and B3LYP/6-31G* calculations on **3** have identified that in the gas phase, the most stable envelope conformation is in the northern hemisphere, namely, E_2 ($P/\pi = 1.9$). The identity of the local minimum in the southern hemisphere depends on the theoretical treatment used. The HF calculations identify ^{2}E ($P/\pi = 0.9$) as the local minimum, while ^{4}E ($P/\pi = 1.3$) is the calculated B3LYP minimum. The preferred C_5-C_4 rotamer is in all cases gg, except ^{2}E (HF) and E_3 (HF), in which the gt rotamer is favored.

(b) Single point energies with the B3LYP/6-31G* optimized geometries of **3** at the B3LYP/6-31+G**, B3LYP/6-311+G**, and B3LYP/6-311+G(2d,2p) were almost identical. Therefore, the 6-31+G** basis set appears to be adequate. While the energies obtained with these three large basis sets were in agreement, for many conformers the energies differed substantially from the B3LYP/6-31G* energies. This observation is in accord with recent work[27−29] that has demonstrated that in order to obtain reliable energies from DFT calculations with carbohydrates, basis sets with diffuse functions must be employed.

(c) Full optimization of the B3LYP/6-31G* geometries of **3** at the B3LYP/6-31+G** level provided energies which are in excellent agreement with the B3LYP/6-31+G** single point energies. Moreover, the bond lengths and bond angles in the B3LYP/6-31G* and B3LYP/6-31+G** optimized geometries were essentially identical.

(d) For some conformers the favored C_5-C_4 rotamer was slightly dependent on the basis set. In particular, for ^{2}E and E_3, the gg rotamer is of the lowest energy at B3LYP/6-31G*, whereas the gt orientation is favored at the B3LYP/6-31+G** level by ∼0.5 kcal/mol.

(e) There is good agreement between the partial potential energy surface for **3** reported here and that derived from molecular mechanics (MM3) by Imberty, Pérez and co-workers.[7a] For the HF/6-31G* surface, agreement is found with respect to the northern and southern minima, although the route of pseudorotation differs. Poorer correlation is observed with the B3LYP/6-31G* surface. However, the single point energies at the B3LYP/6-31+G**, B3LYP/6-311+G**, and B3LYP/6-311+G(2d,2p) levels are in good agreement with the MM3 results.

(f) The B3LYP/6-31G* optimized geometries of **3** have been used to relate various structural parameters with conformation. The trends observed are consistent with previous work[1,13,14,22] on other furanose rings, including **1**.

Acknowledgment. This research has been supported by The Ohio State University and the National Science Foundation (T.L.L.: CHE-9875163 and C.M.H.: CHE-9733457). We acknowledge support from the Ohio Supercomputer Center where some of these calculations were performed. We are grateful for helpful comments from the referees, and we also thank Dr. Alfred D. French for providing us with a program for calculating the Cremer−Pople puckering angles shown in Table 4.

Supporting Information Available: Cartesian coordinates for optimized structures, comparison of gas-phase structures with nucleotide crystal structures, absolute energies, and trend lines for all parameters not provided in the text. This material is available free of charge via the Internet at http://pubs.acs.org.

JO000426W